Bank Interaction Effects on Ships in 6 DOF

G. Delefortrie[1], J. Verwilligen[2], K. Eloot[2], E. Lataire[1]

[1] Ghent University, Belgium

[2] Flanders Hydraulics, Belgium

Abstract

This paper presents the used mathematical formulations to predict ship bank interaction in six degrees of freedom (6 DOF) as applicable in a ship manoeuvring simulator. The mathematical models are based on a comprehensive database (+10,000 model tests carried out in a towing tank) and are capable to cope with a variety of realistic cross sections, based on a limited set of coefficients. Compared to previous publications on bank effects, the lateral force of these bank effects with point of application at the forward perpendicular, is now predicted with an alternative mathematical model that offers the same predictability as the original one, but that better describes the physical background. Moreover, new formulations are included to predict the bank induced components of the ship in the vertical plane (heel, midship sinkage and trim). Although these tend to be neglected, the experimental results show that the effect of confinement and eccentricity can be significant and that a 6 DOF mathematical model is needed for a correct prediction of the manoeuvring behaviour.

A difficulty that is still present is the correct separation of the open water contribution and the contribution due to confinement. This is especially the case for rather high displacement ship models,

such as the KVLCC2 tanker, in the 7m wide towing tank, that even sense the tank walls when being towed on the centreline. This topic will be coped with in future publications, along with an extension for ships that sail with a drift angle.

Keywords

restricted; shallow; confined; mathematical model; model tests; towing tank; ship manoeuvring

List of symbols

A	area	m²
A_{M}	ship's cross section	m²
B	ship's breadth	m
C_{B}	block coefficient	-
C_{M}	ship's cross sectional coefficient	-
D	diameter	m
$d_{2\mathrm{b}}$	ship-bank distance parameter	-
Fr_h	Froude depth number	-
G	position of centre of gravity	
g	gravity acceleration constant	m/s²
h	water depth	m

K	heel moment	Nm
K	position of keel	
L	ship length	m
M	trim moment	Nm
M	position of metacentre	
m	blockage ratio	-
n	propeller rate	1/s
N	yaw moment	Nm
O	origin	-
p	roll rate	deg/s
q	pitch rate	deg/s
r	yaw rate	deg/s
T	ship's draft	m
$Tu_{(m)}$	(modified) Tuck number	-
u	longitudinal speed	m/s
v	lateral speed	m/s
w	vertical speed	m/s
w	wake factor	-
w	weight factor	-

W_0	tank/channel width	m
V	magnitude of the ship's velocity vector	m/s
y_{infl}	influence width for restricted water effects	m
X	longitudinal force	N
x	longitudinal coordinate	m
x_F	centre of floatation	m
Y	lateral force	N
y	lateral coordinate	m
Z	vertical force	N
z	(midship) sinkage; vertical coordinate	m

β	drift angle	deg
Δ	ship's displacement	N
δ	rudder angle	deg
δ	Difference	-
δ_{BLI}	Boundary layer influence thickness	m
ε	propeller advance angle	deg
ξ	regression coefficient	
ϑ	pitch angle	deg

ρ	(water) density	kg/m³
ψ	course angle	deg
χ	weighted area	m²
Ω	cross section of the waterway	m²

Subscripts

0	earth (tank) fixed
A	stern (aft)
Avg	averaged
BANK	the component induced by the presence of a bank
$\mathrm{crit}(1)$	critical (1 = blockage dependent) Froude number
eq	equivalent
F	bow (forward)
G	w.r.t. centre of gravity
H	w.r.t. hull
hyd	hydrostatic
L	longitudinal
lim	limited
M	midship

P	with respect to propeller
PP	between perpendiculars
Ship	at ship
T	w.r.t. thrust; transversal
W	w.r.t. waterplane

Superscripts

‘	non-dimensional; horizontally bound
$*$	apparent
$+$	w.r.t. positive (thrust)

Abbreviations

PS	port side
RANS	Reynolds Averaged Navier Stokes
SS	starboard side
ukc	under keel clearance, expressed as a percentage of the maximal static draft

1 Introduction

Ship bank interaction commonly denotes the phenomenon of hydrodynamic forces that act on the ship created by a disequilibrium of the pressure fields on starboard and portside of a sailing ship. This disequilibrium comes from the presence of a restriction or asymmetry between each of the sides of the ship, in this case a bank or quay wall. Even when sailing on the centreline of a symmetric cross section the hydrodynamic behaviour of the ship changes due to the increased return flow, squeezed within the ship and the limitations of the cross section. These additional hydrodynamic forces alter the behaviour of the ship and should thus be correctly predicted if the aim is to consider them in a ship manoeuvring simulator. The latter can be used either as a tool to adequately design fairways or to provide appropriate training in existing fairways to mitigate the risk of incidents.

The research on ship bank interaction historically focusses on the disequilibrium and consequently on the prediction of the sway force and yawing moment due to the presence of a bank. The number of parameters that affect this phenomenon are basically the ones that affect the flow speed in the gap between a given ship and a bank, namely:

- The velocity of the ship V;
- The space below the keel or under keel clearance, in this article expressed as a percentage of the maximal draft or with the parameter $T/(h-T)$;
- The space in between the bank and the ship or the distance to the bank,
- which in turn depends on the layout of the bank, from a simple linear slope to an irregularly shaped profile.

Especially the latter one is difficult to parametrize and as research on ship bank interaction originated in the mid of the 20th century, the experimental model scale method was at that time the most valuable option to explore. In order to minimize the number of tests, a given cross section was used in the beginning, for instance the Panama canal, as used by Schoenherr (1960) or a trapezoidal section with 1/1 sloped banks by Fujino (1968). In most cases the cross section was simplified by a vertical straight wall, for instance the tank wall or a purposedly built quay wall. Investigations on varying the layout of the bank were performed by Norrbin (1974) and Fuehrer (1978).

Numerical research on ship bank interaction started in the 1960s with the application of potential flow techniques by Newman (1965). Although modern potential flow techniques can fairly well characterize the free surface elevations and vertical motions of the ship, Yuan (2019), the viscous effects on sway force and yaw moment make it less suitable to study ship bank interaction and potential flow techniques are being phased out in favour of RANS or more advanced techniques, see Van Hoydonck et al. (2019).

Due to the numerous parametric variations and the cost of experimental research RANS has taken an important, not to mention dominant, share of the research according to recent literature. Even then the papers tend to focus on a specific topic of ship bank interaction such as the increased resistance when sailing in a cross section. A recent example of such research is presented by Hadi et al. (2023), who first validated their CFD code based on open water resistance test and then used CFD to investigate the increase of resistance due to blockage in a number of cross sections.

In general the study of ship bank interaction is extended towards the horizontal degrees of freedom. Kaidi et al. (2017), studied the effect of propulsion on the surge and sway force and on the yaw moment when sailing eccentrically along a 27° sloped bank.

Lee (2023) conducted a CFD study with two benchmark hulls (KVLCC2 and DTC) near a 1/4 sloped bank (~ 14°). For both ships the results are shown for 6 DOF, but it is a strange fact that the bare hull KVLCC2 has

a bow in moment at large speeds, in contrast to the commonly reported bow out moments during ship bank interaction, for instance by Luo et al. (2021), who tested the KVLCC2 along bank slopes from 4° up to 20°, however, at smaller speeds and neglecting the free surface effect. The discussion is limited to the sway force and yaw moment, but tests were conducted at minor drift angles as well.

Kim and Ng (2017) studied different bank arrangements with different setups of the CFD open source suite OpenFOAM, although the trends of the EFD were well captured, the underprediction was obvious which the author ascribed to the fact that they maintained the ship fixed in the vertical plane during computations. This advocates already for a duly 6 DOF approach.

Liu et al. (2021) discuss that 6 DOF behaviour of the KCS at what they call extreme conditions, namely at high speed (up to $Fr_{h_{\mathrm{crit}}}(m)$), small under keel clearance. Although the CFD study was limited to a vertical quay wall, some insights are provided on how the repulsive bank induced sway force in such extreme conditions can be attributed to the wave elevations along the hull.

All the above papers have in common that a few cases are simulated and a few trends shown which can be resumed as follows:

- Ship-bank interaction is characterized by a lateral attraction force towards the closest bank combined with a bow out moment, an increased resistance and an increased squat. The increase in lateral force is also accompanied by an increase in heel moment. In very shallow waters, the lateral force can become an overall repulsive force directed away from the closest bank but the bow out moment remains.
- A decrease in lateral distance, a decrease in water depth, an increase of velocity and an increase of the slope of the bank (for a given lateral distance), will increase the magnitude of previously described forces.

In contrast with the above topical publications, information about a wider range of trends leading towards the formulation of a mathematical model is more scarce in literature. Schoenherr (1960) published one of the first ship-bank interaction mathematical models. From the early mathematical model publications, Norrbin (1985) is well known, as he proposed a mathematical model for sway force and yaw moment that included the under keel clearance, the bank slope and even the presence of a submerged section of that bank. Although it was dedicated to one ship only, the formulations are still used in ship manoeuvring simulations.

An alternative prediction of the sway force and yaw moment due to the presence of banks was provided by Ch'ng et al. (1993). The novel additions were the consideration of the effects of the thrust and the definition of the ship bank distance at half the draft of the ship.

The fact that the expression of the ship bank distance is the most tedious parameter, as it should be useable for any bank layout, lead to a comprehensive model test program executed in the Towing Tank for Manoeuvres in Confined Water (Flanders Hydraulics, in co-operation with Ghent University), that eventually lead to a new definition of the distance between the ship and the bank.

Based on this research mathematical models have been published for the sway force and yaw moment (Lataire et al, 2018) and for the longitudinal force (Lataire et al., 2015), while Lataire et al. (2016) discussed the squat phenomenon near banks, however, without presenting a mathematical model formulation, although a partial model valid in a rectangular cross section was published previously by Lataire et al. (2012).

The goal of the present paper is to extend the existing mathematical model formulations towards 6 DOF, in particular towards the prediction of heave, trim and heel for a ship that sails on a straight line along a steady bank of any layout. The emphasis is put on the useability for ship manoeuvring simulation, thus robustness, genericity and qualitative trends are prioritized over quantitatively correct spot checks. The

formulations of the ship-bank interaction appear to be valid for the wide range of conditions presented in this paper, but regression coefficients remain ship specific and have a confidential nature. Future researchers are invited to test these formulations with their own data. At the same time, the assumptions and limitations of the mathematical model will be discussed. An important limitation was recently published by Lataire et al. (2023). Due to scale effects, the under keel clearances and distances to the bank should not become too small while performing model scale research. The minimal gap should be larger than the influence of the boundary layer thickness on both sides of the gap. This influence δ_{BLI} depends on the scale of the ship and is typically 8% ukc for a full scale ship, but 26% ukc for a 1 m long ship model.

The main contributions to the state of the art can therefore be summarized as follows:

- To the authors' best knowledge it is the first time that mathematical model formulations are provided to predict the ship-bank interaction in all 6 degrees of freedom when a ship sails along a steady, but not necessarily regular, cross section. Future users can determine their own coefficients for their specific case based on these formulations, or further enhance them.
- It will be shown that the often reported sign reversal of the ship-bank induced sway force at the fore perpendicular can be linked to a critical Froude number, which is related to the available gap the water has below the bow to evacuate. This gap is limited by the sinkage of the ship, which implies that all degrees of freedom need to be considered simultaneously.
- The ship-bank induced roll moment can be merely attributed to the water level drop between ship and bank and thus to a dominant hydrostatic effect.

2 Experimental program

The mathematical models in the present paper are all derived based on captive model tests that have been carried out in the Towing Tank for Manoeuvres in Confined Water (Flanders Hydraulics – co-operation with Ghent University) between 2006 - 2022. This fully automated towing tank has the following dimensions: 80 x 7 x 0.5 m³. A more ample description of its capabilities is available in Delefortrie et al. (2016b). In this paper the results for seven ship models are discussed, of which two were tested at two distinct loading conditions. The main dimensions of these ship models are shown in Table 1.

Table 1 – Considered ship models

Code (year)	**Type**	L_{pp} **(m)**	B **(m)**	T **(m)**	$\frac{\Delta}{g}$ **(ton)**	KM **(m)**	**Scale**
A01 (2010)	Ro-ro (twin rudder, twin propeller)	190.0	31.0	7.4	27185	17.16	50
B01 (2010)	Inland (twin rudder)	108.0	11.4	3.65	4096	5.03	25
C0P (2010)	12,000 TEU	348.0	48.8	15.2	167817	23.91	80
C0U01 (2006)	8,000 TEU	331.3	42.8	14.54	136718	18.53	80.8
C0U03 (2006)				12.0	108838	18.74	
G0M (2006)	Gas tanker	265.6	41.6	11.0	93641	18.84	70
T0Z (2010)	KVLCC2	320.0	58.0	20.8	311378	24.23	75
T0102 (2022)	Bulk carrier	282.0	45.0	12.5	131026	19.64	70
T0103 (2022)				7.0 (F) – 9.0	80948	24.65	

Each ship model was tested in one or more cross sections as depicted in Table 2. A cross section is determined by lateral and vertical boundaries and a water depth. The boundaries are given in model scale coordinates in a clock wise order (column “coordinates” in Table 2). As an example the coordinates of the cross section I are plotted in Figure 1, while the used coordinate systems are shown in Figure 2. The corresponding water levels can be retrieved by the under keel clearances of the different ships tested in such cross section.

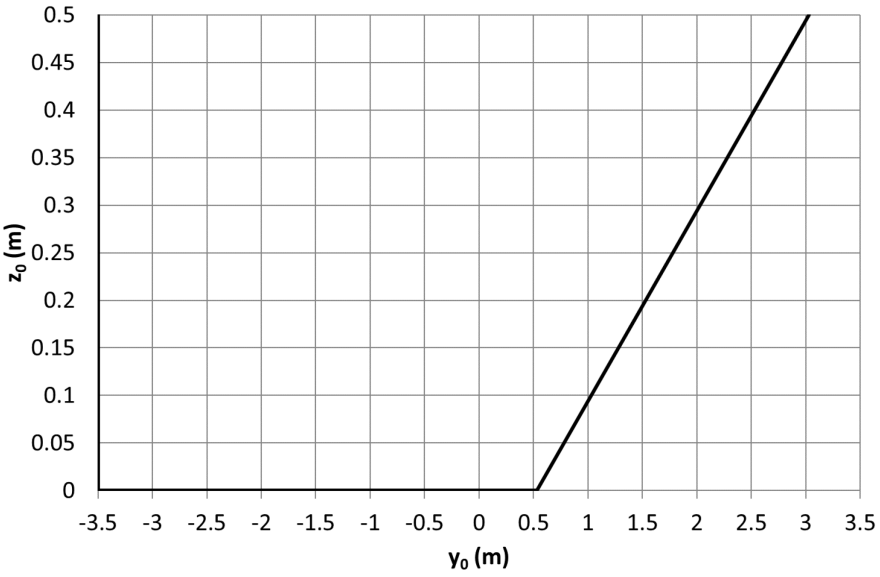

Figure 1 – Example of a cross section (I: 1/5 slope SS [3.03,0.5] [0.53,0] [-3.5,0] [-3.5,0.5] in Table 2)

The captive model test program comprised steady straight line tests (without drift angle) conducted at different eccentricities, forward surge and sway velocities and propeller rates. The eccentricities were usually varied as follows:

- Along the centreline, which is defined as the line that divides the cross section in two equal areas on starboard and on portside;
- Increasing the eccentricity, by decreasing the distance towards the closest bank, which sometimes implied that the ship could sail above a sloped bank or even above a submerged section.

The ship speed was usually varied as follows:

- A minimum speed corresponding to 4 knots full scale
- Increasing the speed in steps of 2 to 4 knots full scale

1

Table 2 – Considered cross sections (116)

Code	Comment	Coordinates	Ships (model scale midship draft m)	ukc
A	Empty tank	[3.5,0.5] [3.5,0] [-3.5,0] [-3.5,0.5]	T0102 (0.179)	100%, 25%, (10%)
			T0103 (0.114)	100%, 25%, (10%)
			A01 (0.148)	(10%) to 120%
			T0Z (0.277)	50%, 35%, (10%)
B	Quay SS	[2.83,0.5] [2.83,0] [-3.5,0] [-3.5,0.5]	C0U01 (0.180)	100%, 35%, (10%)
			C0U03 (0.149)	100%, 35%, (10%)
			G0M (0.157)	70%, 35%
C	Quay PS	[3.5,0.5] [3.5,0] [-2.0,0] [-2.0,0.5]	T0102 (0.179)	100%, 25%, (10%)
			T0103 (0.114)	100%, 25%, (10%)
D	Dock 5B	[1.171,0.5] [1.171,0] [-2.694,0] [-2.694,0.5]	T0Z (0.277)	50%, 35%, (10%)
E	Dock 2.5B	[-0.762,0.5] [-0.762,0] [-2.694,0] [-2.694,0.5]	T0Z (0.277)	50%, 35%, (10%)
F	Dock 1.7B	[-0.762,0.5] [-0.762,0] [-2.694,0] [-2.694,0.5]	T0Z (0.277)	50%, 35%, (10%)
G	Dock 1.25B	[-1.728,0.5] [-1.728,0] [-2.694,0] [-2.694,0.5]	T0Z (0.277)	50%, 35%, (10%)
H	Dock 1.05B	[-1.882,0.5] [-1.882,0] [-2.694,0] [-2.694,0.5]	T0Z (0.277)	50%, 35%, (10%)
I*	1/5 slope SS	[3.03,0.5] [0.53,0] [-3.5,0] [-3.5,0.5]	C0U01 (0.180)	100%, 35%, 12.5%, (10%)
			C0U03 (0.149)	100%, 35%, 15%, (10%)
			G0M (0.157)	70%, 35%
J	1/5 slope submerged SS	[3.5,0.5] [3.5,0.12] [1.13,0.12] [0.53,0] [-3.5,0] [-3.5,0.5]	C0U01 (0.180)	100%, 35%, (10%)
			C0U03 (0.149)	100%, 35%, (10%)
			G0M (0.157)	70%, 35%
K	1/4 slope submerged 1 SS	[3.5,0.5] [3.5,0.15] [1.28,0.15] [0.53,0] [-3.5,0] [-3.5,0.5]	C0U01 (0.180)	100%, 35%, 12.5%, (10%)
			C0U03 (0.149)	100%, 35%, 15%, (10%)
			G0M (0.157)	70%, 35%
L	1/4 slope submerged 2 SS	[2.39,0.5] [2.39,0.15] [1.28,0.15] [0.53,0] [-3.5,0] [-3.5,0.5]	C0U01 (0.180)	35%
M	1/4 slope submerged 3 SS	[1.835,0.5] [1.835,0.15] [1.28,0.15] [0.53,0] [-3.5,0] [-3.5,0.5]	C0U01 (0.180)	35%
N	1/8 slope SS	[3.5,0.5] [3.5,0.371] [0.53,0] [-3.5,0] [-3.5,0.5]	C0U01 (0.180)	100%, 35%, (10%)
			C0U03 (0.149)	100%, 35%, (10%)

Code	Comment	Coordinates	Ships (model scale midship draft m)	ukc
			G0M (0.157)	70%, 35%
O	1/8 slope SS submerged	[3.5,0.5] [3.5,0.15] [1.73,0.15] [0.53,0] [-3.5,0] [-3.5,0.5]	C0U01 (0.180)	100%, 35%, (10%)
			C0U03 (0.149)	100%, 35%, (10%)
			G0M (0.157)	70%, 35%
P	1/3 slope SS	[3.5,0.5] [3.5,0.423] [2.23,0] [-3.5,0] [-3.5,0.5]	C0U01 (0.180)	100%, 35%, (10%)
			C0U03 (0.149)	100%, 35%, (10%)
			G0M (0.157)	70%, 35%
Q	Quay PS 1/4 slope SS	[3.5, 0.45] [1.7,0] [-2.7, 0] [-2.7, 0.45]	A01 (0.148)	100%, 35%, (10%)
			B01 (0.146)	195%, 35%, 20%
			C0P (0.190)	100%, 35%, (10%)
			T0Z (0.277)	50%, 35%, (10%)
R	1/1 slope PS 1/3 slope SS	[3.05, 0.45] [1.7, 0] [-2.5, 0] [-2.95, 0.45]	A01 (0.148)	100%, 35%, (10%)
			B01 (0.146)	195%, 35%, 20%
			C0P (0.190)	100%, 35%, (10%)
			T0Z (0.277)	50%, 35%, (10%)

*plotted as example in Figure 1

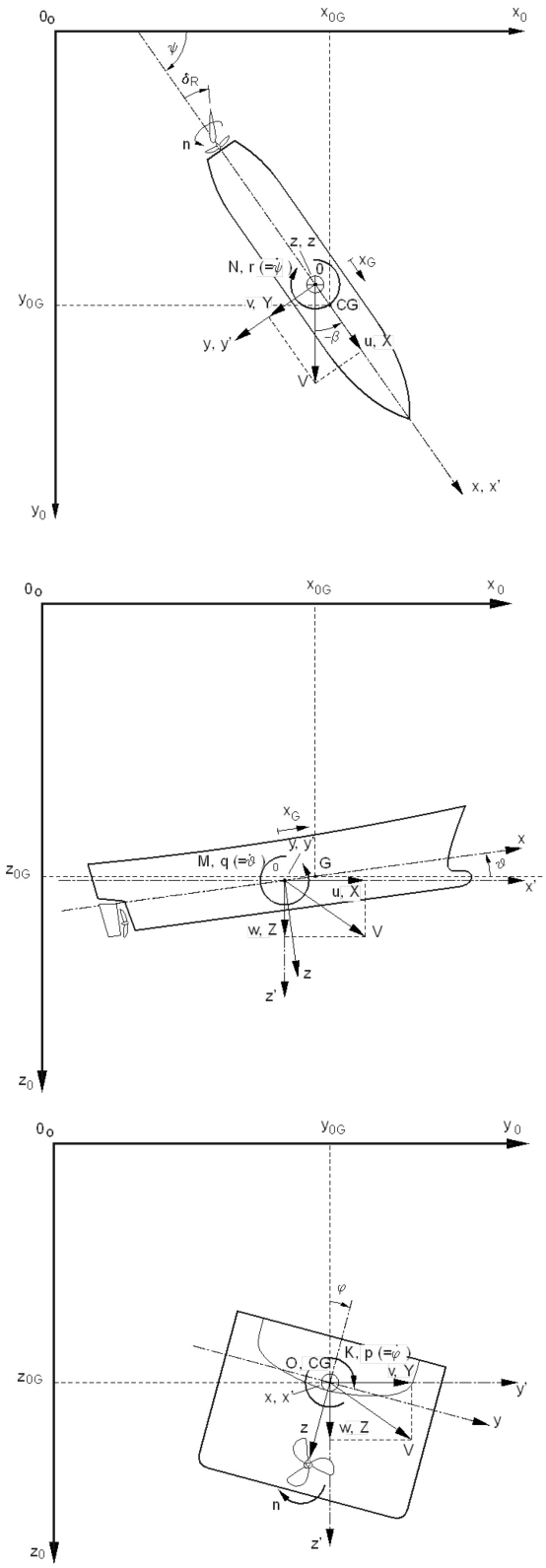

Figure 2 –Ship and earth fixed coordinate systems in 6 degrees of freedom: projections on the $\boldsymbol{x_0y_0}$-plane, $\boldsymbol{y_0z_0}$-plane and $\boldsymbol{z_0x_0}$-plane.

The maximal speed was never larger than the theoretical critical speed that considers the blockage m , or the ratio of the wetted cross section of the ship to the cross section of the fairway. It can be proven that this critical speed is (Delefortrie et al., 2024):

$$Fr_{h,\text{crit}} = \left(2\sin\left(\frac{\arcsin(1-m)}{3}\right)\right)^{3/2} \quad (1)$$

The propeller rates were either at the model self-propulsion point that corresponded to the equivalent speed in absence of the banks or either zero (propeller shaft fixed at 0 rpm).

Although variations of rudder angle and drift angle were included in the test program, these are not yet covered by the mathematical model formulations of the present paper. However, these contributions can be summarized as follows:

- The drift angle has a significant effect as it combines low/high pressure zones around the ship (depending on the drift attitude) with the low pressure zone in between ship and bank. A discussion on this topic was recently published by the authors (Delefortrie et al., 2023). As it requires further study, the effect of drift is not yet included in the present mathematical model.
- The effect of the bank on the rudder induced forces is only significant when the ship sails very close to the bank (a few meters at full scale) and has no impact when half a beam or further separation between ship and bank.

During the model tests the following values were measured:

- The total longitudinal force acting on the ship (N)
- The sway force acting on the ship (N), measured along two longitudinal positions, which can be recomputed to:
    - A total sway force (N)

    - A yawing moment (Nm)
- The sinkage of the ship at four positions along the hull, which can be recomputed to
    - A midship sinkage (m)
    - A trim (mm/m or deg)
- The heel moment (Nm), but not for all ship models
- Thrust (N) and propeller shaft torque (Nm)
- Longitudinal and lateral force acting on the rudder (N) along with steering torque (Nm)

3 Result trends for experiments

Figure 3 shows the main physical process that governs the ship bank interaction phenomenon. Due to the more limited space the return flow has to accelerate more in between the ship and the nearest bank (Figure 3a). Because of the Bernoulli principle, the pressure drop will also be stronger in between the ship and the nearest bank. As a result the midship depression will increase, with a resulting force vector (depicted in white in Figure 3b) that attracts the ship towards the bank, hence the historical naming of the phenomenon as bank suction. For moderate conditions, the ship bank interaction will always cause:

- A resistance increase in the longitudinal direction.
- A sway force directed towards the closest bank. The resultant is located in the aft part of the ship, hence creating a yaw moment that direct the bow away from the closest bank.
- An increase of the squat of the ship, i.e. increased midship sinkage and altered trim behaviour.
- A heel of the ship so that the upper part of the ship heels towards the closest bank.

While the force indicated in Figure 3 would create a heel of the ship oriented so that the upper part moves away from the closest bank, this moment is overruled by the result of the hydrostatic imbalance between

both sides of the ship which creates a much larger moment so the top side of the ship heels towards the bank.

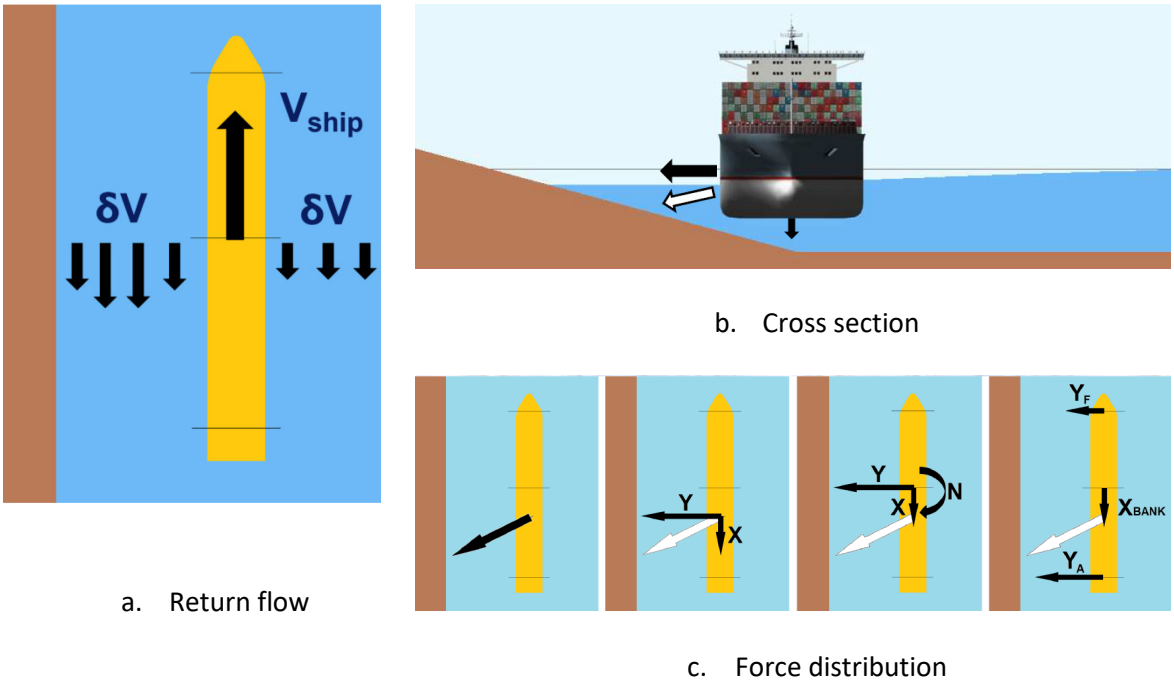

a. Return flow

b. Cross section

c. Force distribution

Figure 3 – Physical process of ship bank interaction

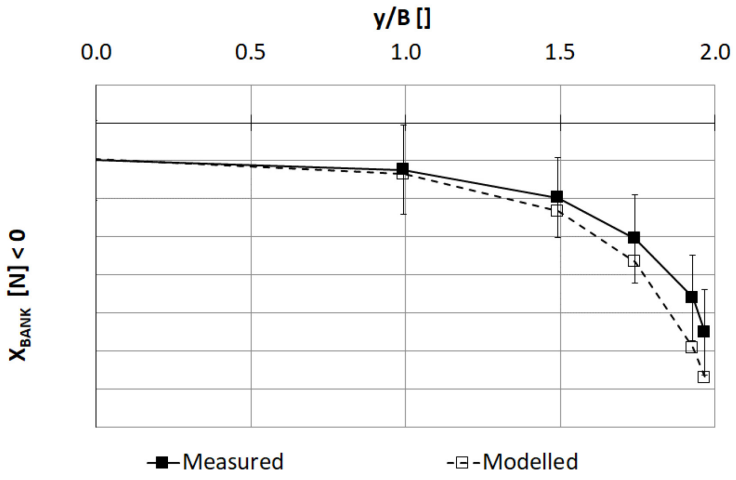

Figure 4 – Influence of the lateral position on the longitudinal bank effect X_{BANK} of T0Z in the rectangular cross section D, 50% ukc, 8 kn full scale speed, propeller rpm at 8 kn open water self-propulsion. The measured values are according to equation (8), while the modelled are according to equation (51).

Figure 4 shows how the longitudinal force increases with decreasing distance towards the closest bank. As the test was conducted at self-propulsion in open water, the actual force that is shown is to be attributed to the fact that one is sailing in a confined section, so even on the centreline an increase of resistance is seen.

Uncertainty intervals have been plotted on the measurements. The uncertainty assessment has been based on the appropriate ITTC guideline (ITTC, 2021). Although this guideline is very comprehensive it does not cover uncertainties induced by the built-in cross sections, which would require Monte-Carlo simulations with the obtained mathematical models. The uncertainty intervals presented in this paper have been derived based on the major sources of uncertainty, which depend on the degree of freedom:

- The noise uncertainty for the surge force;
- The rail alignment and measurement resolution for the heave and pitch;
- The repeatability uncertainty for the other degrees of freedom.

Figure 5 visualises the ship bank induced sway force and yaw moment for a variety of under keel clearances at a fixed eccentricity and speed. The bank induced yaw moment is always directed away from the bank and its magnitude tends to increase monotonically with decreasing under keel clearance. This monotonic behaviour is not seen for the sway force. The reason for this is better seen when splitting the total sway force and yaw moment as a sway force at the fore perpendicular and a sway force at the aft perpendicular:

$$Y_F = \frac{Y}{2} + \frac{N}{L_{PP}} \tag{2}$$

$$Y_A = \frac{Y}{2} - \frac{N}{L_{PP}} \tag{3}$$

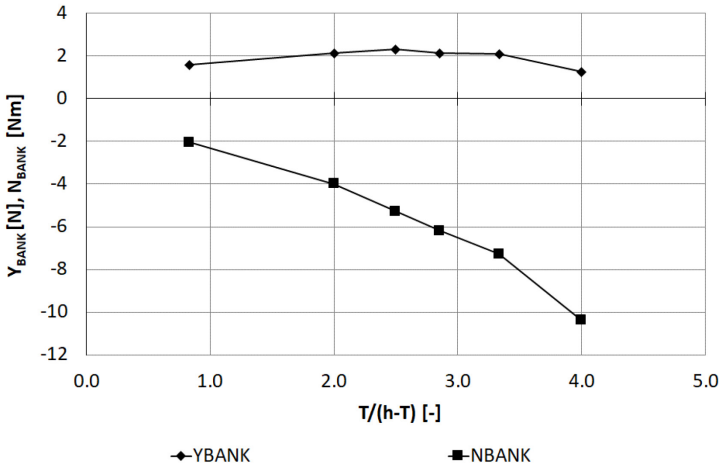

79

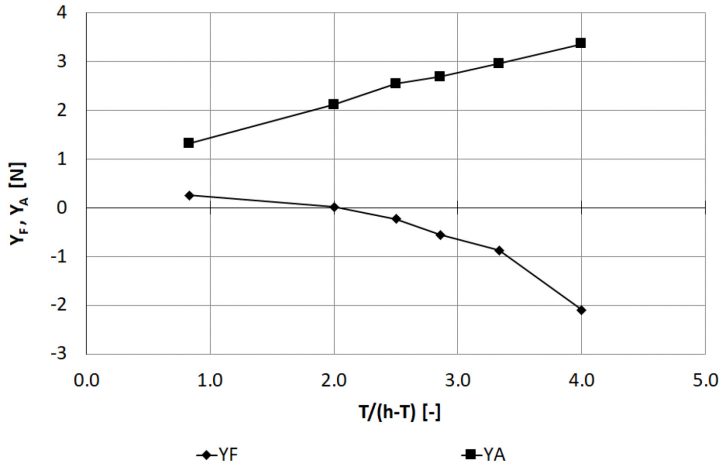

80

81 *Figure 5 – Lateral force and yaw moment (top) or lateral force at the fore and aft perpendicular (bottom) for a wide range of*
82 *water depths (here expressed as the ratio (T/(h-T)) for ship model A01, in the FH towing tank (cross section A) at lateral position*
83 y_0 *=2.5 m, according to 10 knots full scale, fixed propeller shaft 0 rpm. A positive sway force means an attraction towards the*
84 *closest bank. The uncertainty intervals are smaller than the size of symbols.*

85

86 The latter Y_A is a continuously increasing suction force with decreasing water depth, whereas the former
87 Y_F changes from a suction force towards a repulsive force at smaller under keel clearances. At some point
88 the repulsive force at the fore can dominate the suction force at the aft, resulting in a total repelling sway
89 force. For these reasons the ship bank interaction is modelled for Y_F and Y_A.

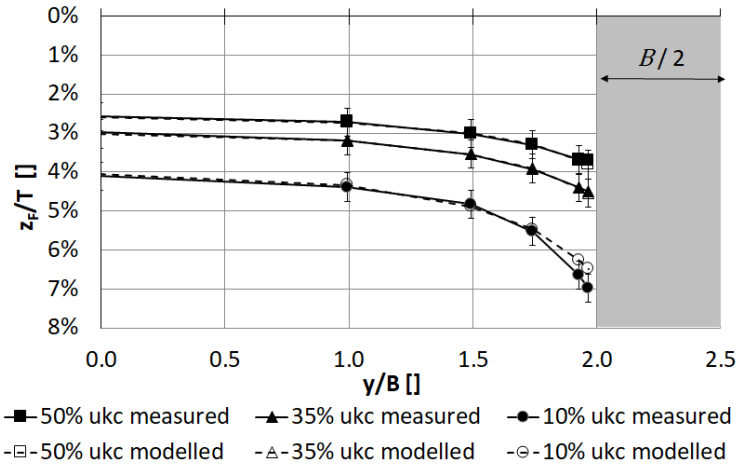

Figure 6 – The measured and modelled running sinkage at the FP of ship T0Z for a wide range of lateral positions in a canal width of 5B (cross section D) and at 8.0 knots full scale

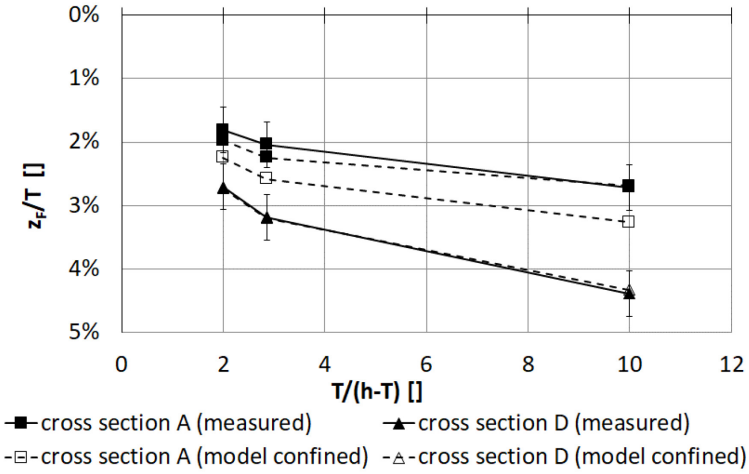

Figure 7 – The measured and modelled running sinkage at the FP of ship T0Z sailing at the centreline of a canal width of 5B (cross section D) or 9B (cross section A) at different water depths and at 8.0 knots full scale

Figure 6 demonstrates how the ship's sinkage is affected by the eccentricity. The sinkage as measured at the fore perpendicular is taken as an example, but the same is true for the sinkage at the aft perpendicular. As for the longitudinal force, not only an increase with decreasing lateral distance towards the closest bank is seen, but according to Figure 7, also an increase of sinkage due to the confinement of the section, in other words, the sinkage when sailing along the centreline is already larger compared to the sinkage

when the ship would sail at the same velocity and water depth in a laterally unrestricted environment (here 9/5 wider tank).

Finally, Figure 8 shows how the heel moment of the ship evolves with decreasing distance from the bank. The evolution is quite similar to the evolution of the total sway force. In fact if a vertical application arm of the sway force is computed, it seems quite constant for significant force and moment magnitudes. Nevertheless, the actual physics behind this process is the dominant hydrostatic contribution of the heel moment.

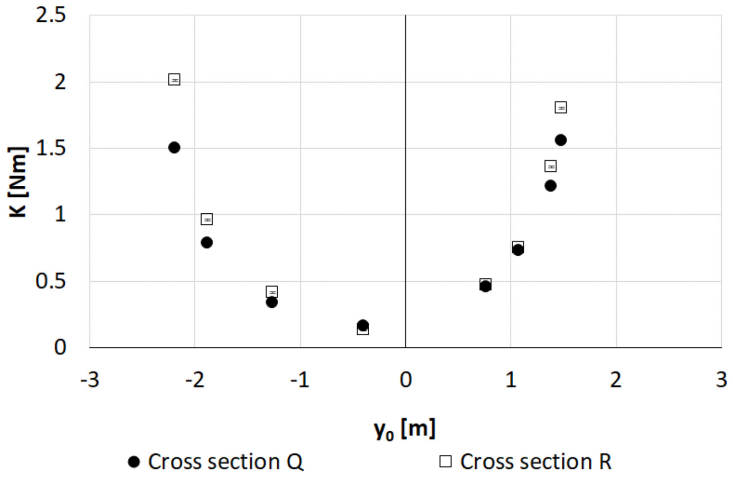

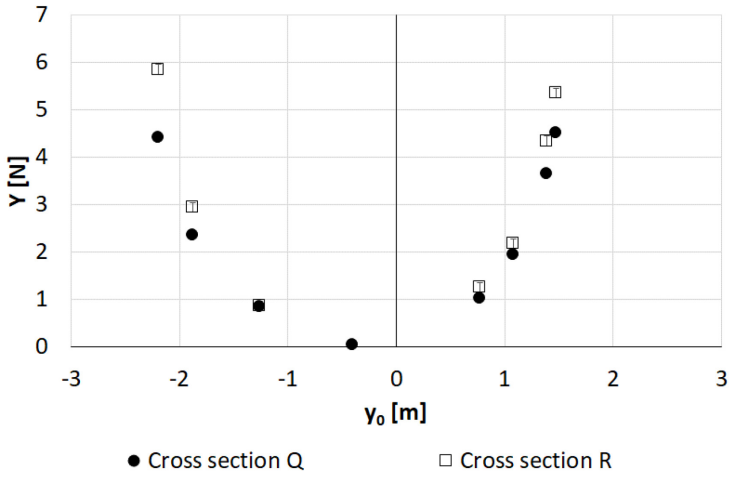

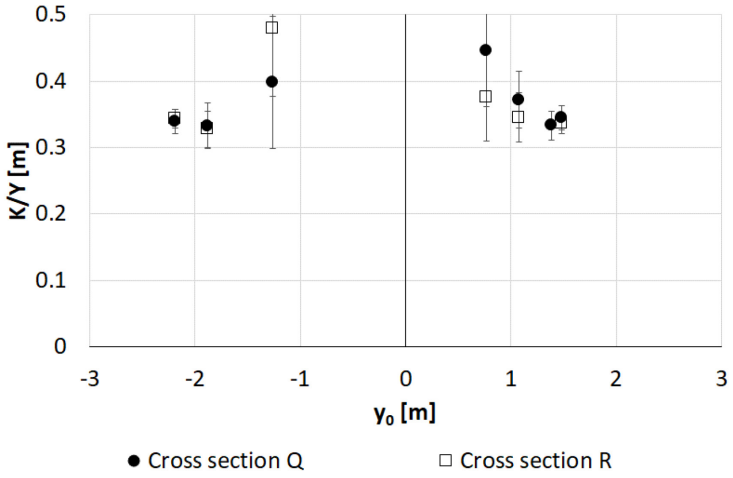

Figure 8 – The measured heel moment and sway force for ship A01 in cross sections Q and R (see Table 2), 35% ukc, 8.0 knots full scale, fixed propeller shaft 0 rpm. Irrespective y_0 the closest bank is always located on the starboard side of the ship

From the shown examples it is clear that all degrees of freedom are affected by the presence of the banks. A major distinction exists between the longitudinal force and the squat on one hand and the sway force, yaw and heel moments on the other hand. The former are already affected by the cross section when sailing on the centreline, whereas the latter not, at least when the ship sails on a straight line (without drift angle).

4 Mathematical model

4.1 Overview

The scope of the paper is the formulation of a mathematical model for the hydrodynamic forces originated from the ship bank interaction when a ship sails on a straight line, without use of the rudder. In the case there are no lateral restrictions, the ship will already be subject to a longitudinal force (the balance between the resistance of the ship and the propulsive force) and to heave and trim (the squat). At the

same time any sway force, yaw moment or heel moment is theoretically absent, although the propeller may induce a slight asymmetry. It is therefore important to consider the open water behaviour of the ship and to subtract that behaviour from the measured forces during ship bank interaction to have the contribution of the latter.

4.2 Open water manoeuvring model

The open water behaviour of the ship in terms of longitudinal force is based on Delefortrie et al. (2016a), whereas for the squat the mathematical formulation from Delefortrie et al. (2022) is used. To set the ideas the formulations are outlined here as well.

The longitudinal force in open water consists of a part attributed to the hull, the propeller and the rudder.

$$X_{\mathrm{H}} = \frac{1}{2}\rho L T V^2 X'(\beta = 0) \tag{4}$$

$X'(\beta = 0)$ represents the regression coefficient for a drift angle equal to zero. A similar formulation is used for the other open water regression coefficients further introduced in this section. The thrust generated by the propeller depends on the advance angle ε

$$\varepsilon = \arctan\left(\frac{(1 - w_{\mathrm{T}})u}{0.7\pi n D_{\mathrm{P}}}\right) \tag{5}$$

$$T_{\mathrm{P}} = \frac{0.7^2}{8}\pi^3 \rho n^2 D_{\mathrm{P}}^4 C_{\mathrm{T}}(\varepsilon)(1 + \tan^2 \varepsilon) \tag{6}$$

Because of thrust deduction, only part of the thrust of each propeller i is transferred to overcome the resistance

146 $$X_{\mathrm{P}} = \sum \left(1 - t(\varepsilon_i^*)\right) T_{\mathrm{P}i} \quad (7)$$

147

148 Where ε^* is the apparent advance angle (when the wake is neglected or w_T = 0). As in this case the rudder
149 is not used, the minor rudder drag at 0° rudder angle is not separated from the hull resistance. From the
150 measured X the bank induced component is then obtained as:

151

152 $$X_{\mathrm{BANK}} = X - X_{\mathrm{H}} - X_{\mathrm{P}} \quad (8)$$

153

154 For the heave and trim, the measured midship sinkage z and trim θ are first transformed to a heave force
155 and trim moment according to the principle of hydrostatic equilibrium during manoeuvring:

156

157 $$Z_{\mathrm{hyd}} = -\rho g A_{\mathrm{W}} (z + x_{\mathrm{F}} \theta) \quad (9)$$

158 $$M_{\mathrm{hyd}} = -\Delta \overline{GM}_L \theta - \rho g A_{\mathrm{W}} x_{\mathrm{F}} z \quad (10)$$

159

160 For subcritical speeds in open water, the sinkage and trim are proportional with the so-called Tuck number
161 (Tuck, 1966):

163 $$Tu_h = \frac{Fr_h^2}{\sqrt{1 - Fr_h^2}} \quad (11)$$

162

164 expressed as a function of the depth-related Froude number:

$$Fr_h(V) = \frac{V}{\sqrt{g h_{\text{ship}}}} \tag{12}$$

h_{ship} is the local water depth at the ship, so that

$$h_{\text{ship}} = \frac{\Omega_{\text{ship}}}{B} \tag{13}$$

with Ω_{ship} the local cross section of the fairway limited to the breadth of the ship:

$$\Omega_{\text{ship}} = \int_0^h \int_{-0.5\text{B}}^{0.5\text{B}} d\Omega \tag{14}$$

In a steady state condition, meaning that the ship is sailing at constant V and the squat is steady, the vertical position is determined by the equilibrium:

$$Z_{\text{hyd}} + \Delta T u_h Z'(\beta = 0) = 0 \rightarrow Z_{\text{H}} = \Delta T u_h Z'(\beta = 0) \tag{15}$$

$$M_{\text{hyd}} + \Delta L T u_h M'(\beta = 0) = 0 \rightarrow M_{\text{H}} = \Delta L T u_h M'(\beta = 0) \tag{16}$$

The above does not take account of the propeller rate. The effect of the propeller(s), delivering a positive thrust (or turning ahead) is added as follows:

$$Z_{\mathrm{P}} = Z_{\mathrm{PT}}(\beta = 0) T u_h \sum T_{\mathrm{P}i} \tag{17}$$

$$M_{\mathrm{P}} = M_{\mathrm{PT}}(\beta = 0) L \sum T_{\mathrm{P}i} \tag{18}$$

From the total computed Z and M the bank induced components are then obtained as:

$$Z_{\mathrm{BANK}} = Z - Z_{\mathrm{H}} - Z_{\mathrm{P}} \tag{19}$$

$$M_{\mathrm{BANK}} = M - M_{\mathrm{H}} - M_{\mathrm{P}} \tag{20}$$

Similarly to the sway force and the yaw moment, the heave force and pitch moment can be expressed as a heave force at the forward and at the aft perpendicular.

For the sway force, heel and yaw moment, the open water contributions of the hull may be marginal when sailing at zero drift angle, but they are included for reasons of completeness. The hull contribution is as follows:

$$Y_{\mathrm{H}} = \frac{1}{2} \rho L T V^2 Y'(\beta = 0) \tag{21}$$

$$K_{\mathrm{H}} = \frac{1}{2} \rho L T^2 V^2 K'(\beta = 0) \tag{22}$$

$$N_{\mathrm{H}} = \frac{1}{2} \rho L^2 T V^2 N'(\beta = 0) \tag{23}$$

whereas the contribution from the propeller(s) follows from:

$$Y_{\mathrm{P}} = Y_{\mathrm{PT}}^{+}(\beta = 0) \sum T_{\mathrm{P}i} \tag{24}$$

$$K_{\mathrm{P}} = K_{\mathrm{PT}}^{+}(\beta = 0) T \sum T_{\mathrm{P}i} \tag{25}$$

$$N_{\mathrm{P}} = N_{\mathrm{PT}}^{+}(\beta = 0) L \sum T_{\mathrm{P}i} \tag{26}$$

From the total measured Y, K and N the bank induced components are then obtained as:

$$Y_{\mathrm{BANK}} = Y - Y_{\mathrm{H}} - Y_{\mathrm{P}} \tag{27}$$

$$K_{\mathrm{BANK}} = K - K_{\mathrm{H}} - K_{\mathrm{P}} \tag{28}$$

$$N_{\mathrm{BANK}} = N - N_{\mathrm{H}} - N_{\mathrm{P}} \tag{29}$$

4.3 Weighting of the cross section

The pillar of the previously published research is the establishment of the so-called influence width, accepted by the ITTC:

$$y_{\mathrm{infl}} = 5B(Fr_h + 1) \tag{30}$$

which indicates at which horizontal distance from the ship's centreline, an obstacle should be in order to be considered as having a negligible effect on the ship. As such this equation gives a limit for restricted water effects. If nothing is within the influence width, then the measured forces and moments should be the open water forces. For some ship models, such as the KVLCC2 present in this paper, this means that even in an empty towing tank the ship will sense already the walls and that the so-called open water

manoeuvring model presented in the previous section is not a true open water model, but may already be biased by the presence of the tank walls.

This influence width is then used together with the draft of the ship to perform a weighted evaluation of the cross section in horizontal, respectively vertical direction. Each water particle at coordinates (y, z) with respect to the ship has a weight:

$$w = e^{-\left(\xi_y \frac{|y|}{y_{\text{infl}}} + \xi_z \frac{|z|}{T}\right)} \tag{31}$$

ξ_y and ξ_z are calibration coefficients which are determined based on the outcome of the tests and which are constants for each ship-draft combination, but not necessarily for each degree of freedom. This is because not all degrees of freedom are equally sensitive to the lateral or vertical restriction. For instance, the sinkage of the ship is the degree of freedom that will first sense a lateral restriction, hence a different weight is needed.

An integration of the cross section at both sides of the vessel (SS and PS) can be calculated with equations (32) and (33). Here the weight factor can be seen as a (ship dependent) overlay sheet which is placed on the cross section under consideration. All 'water particles' are taken into account, also the particles at a distance far away from the vessel but the weight value for these particles will be insignificant.

$$\chi_{\text{SS}} = \int_0^h \int_0^{y_s} e^{-\left(\xi_y \frac{|y|}{y_{\text{infl}}} + \xi_z \frac{|z|}{T}\right)} \, dy \, dz \tag{32}$$

$$\chi_{\mathrm{PS}} = \int_0^h \int_0^{y_{\mathrm{p}}} e^{-\left(\xi_y \frac{|y|}{y_{\mathrm{infl}}} + \xi_z \frac{|z|}{T}\right)} dy\, dz \tag{33}$$

To avoid misunderstanding: y_{infl} is a constant boundary during integration, evaluated at h. ξ_y lies in a range between 0.1 and 10. , whereas ξ_z is a constant for all environments, degrees of freedom and ships. The sensitivity of the above integrals with the calibration coefficients ξ_y and ξ_z is a function of the integral boundaries, in other words the calibration coefficients ξ_y and ξ_z depend on the size of the cross section, and more specifically a tank bias cannot be excluded. Nevertheless, this does not mean that the concept is not generally applicable, it just implies a tight relationship of ξ_y and ξ_z with the tank dimensions.

For a ship, or an open section (e.g. an ocean), the integrals can be solved as follows:

$$\chi_{\mathrm{ship}} = 2\int_0^T \int_0^{B/2} e^{-\left(\xi_y \frac{|y|}{y_{\mathrm{infl}}} + \xi_z \frac{|z|}{T}\right)} dy\, dz = 2\frac{y_{\mathrm{infl}}\, T}{\xi_y \xi_z}\left(1 - e^{-\frac{\xi_y B}{2y_{\mathrm{infl}}}}\right)\left(1 - e^{-\xi_z}\right) \tag{34}$$

$$\chi_{\mathrm{ocean}} = 2\int_0^\infty \int_0^\infty e^{-\left(\xi_y \frac{|y|}{y_{\mathrm{infl}}} + \xi_z \frac{|z|}{T}\right)} dy\, dz = 2\frac{y_{\mathrm{infl}}\, T}{\xi_y \xi_z} \tag{35}$$

The integrals have thus always a finite solution.

The weighted blockage of half the ship in the portside or starboard side of the section is respectively:

$$\frac{\frac{\chi_{\text{ship}}}{2}}{\chi_{\text{PS}}}; \frac{\frac{\chi_{\text{ship}}}{2}}{\chi_{\text{SS}}} \tag{36}$$

This is then used to define a dimensionless distance to bank parameter $d_{2\text{b}}$:

$$d_{2\text{b}}{}^{-1} = \frac{\frac{\chi_{\text{ship}}}{2}}{\chi_{\text{SS}}} - \frac{\frac{\chi_{\text{ship}}}{2}}{\chi_{\text{PS}}} \tag{37}$$

and an equivalent blockage:

$$m_{\text{eq}} = \frac{1}{2}\left(\frac{\frac{\chi_{\text{ship}}}{2}}{\chi_{\text{SS}}} + \frac{\frac{\chi_{\text{ship}}}{2}}{\chi_{\text{PS}}}\right) - \frac{\chi_{\text{ship}}}{\chi_{\text{ocean}}} \tag{38}$$

This equivalent blockage becomes zero in an open and deep water section by subtraction of $\frac{\chi_{\text{ship}}}{\chi_{\text{ocean}}}$.

When plotting the measurements for a given ship sailing at a given speed in different cross sections it is possible to establish the following relationships:

$$Y_F \propto d_{2\text{b}}{}^{-1};\ Y_A \propto d_{2\text{b}}{}^{-1} \tag{39}$$

$$Z \propto m_{\text{eq}};\ M \propto m_{\text{eq}} \tag{40}$$

$$X \propto m_{\text{eq}}^2 \tag{41}$$

An example is shown in Figure 9.

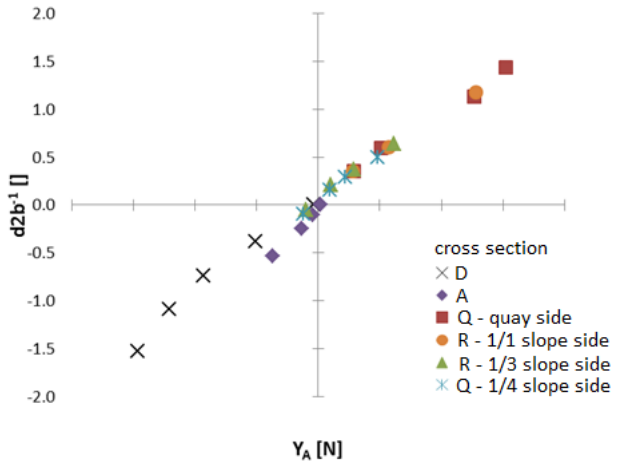

Figure 9 – Relationship between Y_A and $d_{2b}{}^{-1}$ for ship T0Z sailing in different cross sections at 10 knots prototype speed in self-propelled conditions, 50% ukc. The figure is adapted from Lataire (2014).

The above relationships basically select the calibration values ξ_y and ξ_z.

4.4 Effect of water depth, speed and propulsion

For a given distance to bank, the influence of the forward speed of the vessel and water depth should be included. The water depth is very straightforward when a ship sails over a perfectly flat and horizontal bottom. If the bathymetry is more irregular the water depth is not that easy to define. Referring to section 4.2, the Tuck number $Tu_h(Fr_h)$ could be used to model the speed at a given water depth, including the effect of the blockage factor. In infinitely wide cross sections this blockage factor tends to zero and for this reason the bathymetry at a lateral distance beyond y_{infl} from the vessel should not be taken into account. For this reason the cross section of the channel should be defined as:

$$\Omega = \int_0^h \int_{-y_{\text{infl}}}^{y_{\text{infl}}} d\Omega \tag{42}$$

and a limited blockage factor is introduced:

$$m_{\mathrm{lim}} = \frac{A_{\mathrm{M}}}{\Omega} \tag{43}$$

Although this limited blockage factor fits in the concept of the influence width it has a major disadvantage, namely in unrestricted water its value will not be equal to zero. As such, a cross section wider than y_{infl} at both sides of the vessel, will have the same blockage as an infinitely wide shallow ocean. The first critical Froude number should be written then as:

$$Fr_{h,\mathrm{crit1}} = \left(2\sin\left(\frac{\arcsin(1-m_{\mathrm{lim}})}{3}\right)\right)^{3/2} \tag{44}$$

This dimensionless speed can and should be made dimensional by multiplying by $\sqrt{gh_{\mathrm{avg}}}$. This water depth h_{avg} is the ratio between the (limited) cross section area Ω and the width on the free surface W_0, which is the summation of the width on the free surface at the port and starboard side of the vessel (measured from the centre line of the vessel) and limited to y_{infl} on each side of the vessel.

$$h_{\mathrm{avg}} = \frac{\Omega}{W_0} \tag{45}$$

The Tuck number can now be adapted with the updated limit for subcritical speed:

315

316
$$Tu_m(Fr_h) = \frac{{Fr_h}^2}{\sqrt{Fr_{h,\mathrm{crit1}}^2 - {Fr_h}^2}} \tag{46}$$

317

318 A propeller generating thrust pushing the ship forward, accelerates the water flow passing the propeller
319 disk. Therefore the velocity of the water between bank and ship increases and thus decreases the pressure
320 on that part of the hull surface. The influence of the propeller action can be modelled as a partial increase
321 of the forward speed of the vessel by adding a part of the induced velocity in the slipstream at infinity
322 according to the actuator disk theory (V_T):

323

324
$$V_T = \mathrm{sign}(T_\mathrm{P}) \sqrt{\frac{|T_\mathrm{P}|}{\frac{1}{2}\rho\pi\frac{D^2}{4}}} \tag{47}$$

325

326 When the ship model is towed in a towing tank with a forward speed and with propeller rate 0 rpm the
327 axial force as measured on the propeller shaft (T_P) will take a small negative value (increased resistance).
328 To be able to calculate negative values for V_T the absolute value of T_P is used under the root and the root
329 is multiplied by the sign of the thrust ($V_T = 0$ when $T_\mathrm{P} = 0$). This enables then to define an equivalent
330 speed:

332
$$V_\mathrm{eq} = V + \xi_{VT} V_T \tag{48}$$

331

The coefficient ξ_{VT} takes a value between 0 and 1. For the lateral force at the forward perpendicular this coefficient $\xi_{VT,\mathrm{F}}$ is a much smaller value than $\xi_{VT,\mathrm{A}}$ for the lateral force at the aft perpendicular for the same ship.

Only the thrust delivered by the propeller closest to the nearest bank is taken into account in case of a twin screw vessel. Both the Froude and the Tuck number can now be expressed with the equivalent velocity:

$$Tu_m(V_{\mathrm{eq}}) = \frac{{Fr_h}^2(V_{\mathrm{eq}})}{\sqrt{Fr_{h,\mathrm{crit1}}^2 - {Fr_h}^2(V_{\mathrm{eq}})}} \tag{49}$$

And a proportional relation is found between this Tuck number and the lateral bank induced forces:

$$Y_{\mathrm{F}} \propto Tu_m(V_{\mathrm{eq}});\ Y_{\mathrm{A}} \propto Tu_m(V_{\mathrm{eq}}); X \propto Tu_m(V_{\mathrm{eq}}); Z \propto Tu_m(V_{\mathrm{eq}}); M \propto Tu_m(V_{\mathrm{eq}}) \tag{50}$$

which yields the following ship-bank interaction formulations:

$$X_{\mathrm{BANK}} = \xi_X \Delta m_{\mathrm{eq},X}^2 Tu_m(V_{\mathrm{eq},X}) \tag{51}$$

$$Y_{\mathrm{A,BANK}} = \xi_{Y_A} {\Delta d_{2\mathrm{b}}}^{-1} Tu_m(V_{\mathrm{eq},Y_A}) \tag{52}$$

$$Z_{\mathrm{BANK}} = \xi_Z \Delta m_{\mathrm{eq},Z} Tu_m(V_{\mathrm{eq},Z}) \tag{53}$$

$$M_{\mathrm{BANK}} = \xi_M \Delta \mathrm{L_{PP}} m_{\mathrm{eq},M} Tu_m(V_{\mathrm{eq},M}) \tag{54}$$

Specific subscripts were added to the equivalent speeds and blockages to highlight the fact that different regression coefficients are needed for the different degrees of freedom.

The latter two can alternatively be modelled as:

$$Z_{\mathrm{F,BANK}} = \xi_{Z_{\mathrm{F}}} \Delta m_{\mathrm{eq},Z_{\mathrm{F}}} Tu_m\left(V_{\mathrm{eq},Z_{\mathrm{F}}}\right) \tag{55}$$

$$Z_{\mathrm{A,BANK}} = \xi_{Z_{\mathrm{A}}} \Delta m_{\mathrm{eq},Z_{\mathrm{A}}} Tu_m\left(V_{\mathrm{eq},Z_{\mathrm{A}}}\right) \tag{56}$$

For $Y_{\mathrm{F,BANK}}$ a distinction is needed to cover the suction force at larger water depths transforming into a repelling force at smaller water depths. This transition is speed and water depth dependent and was modelled as follows (Lataire et al. (2018)):

$$Y_{\mathrm{F,BANK}} = \begin{cases} \dfrac{T}{h_{\mathrm{ship}} - T} \leq \xi_{hT} & \xi_{Y_F} \Delta \; d_{2\mathrm{b}}^{-1} \;\; Tu_m\left(V_{\mathrm{eq},Y_F}\right) \\ \dfrac{T}{h_{\mathrm{ship}} - T} > \xi_{hT} & \xi_{Y_F} \Delta \; d_{2\mathrm{b}}^{-1} \;\; Tu_m\left(V_{\mathrm{eq},Y_F}\right) \left(1 - \dfrac{Fr^2}{{\xi_h}^2}\left(\dfrac{T^2}{\left(h_{\mathrm{ship}} - T\right)^2} - {\xi_{hT}}^2\right)\right) \end{cases} \tag{57}$$

The above equation, used until presently, does not lead to appropriate results for all cases. The main reason seems to be the lack of inclusion of the effect of the forward sinkage. Therefore a new model formulation is proposed here.

The physical explanation of the lateral force at the bow becoming repulsive is presumed that at some point the flow cannot evacuate anymore below the keel of the ship and accumulates in between the bow and the nearest obstacle, creating the repulsive force. The available space below the bow is:

$$\mathrm{ukc,F} = h_{\mathrm{ship}} - T - z_{\mathrm{F}} \tag{58}$$

Through that space a flow with minimum velocity V needs to be evacuated. The evacuation becomes more difficult with increasing ratio of a Froude number that takes into account water depth, draft and running sinkage at the fore:

$$Fr_{\mathrm{ukc,F}} = \frac{V}{\sqrt{g\left(h_{\mathrm{ship}} - T - z_{\mathrm{F}}\right)}} \tag{59}$$

At some $Fr_{\mathrm{ukc,F,crit}}$ not all of the needed flow can be evacuated below the keel, yielding a pressure increase and thus a repulsive force component.

This is illustrated with the data of Figure 5, which is here repeated in a tabular format (Table 3). The lateral force at the aft perpendicular Y_{A} shows a consistent increase, proportional to the ratio $\frac{T}{h_{\mathrm{ship}}-T}$, whereas the lateral force at the forward perpendicular can only be considered a pure suction force at the largest water depth. Y_{F} decreases in less deep water and becomes repulsive at smaller water depths. For these six model tests at the same speed, propeller rate, eccentric distance in the towing tank but different water depths, the Froude number based upon the net under keel clearance $Fr_{\mathrm{ukc,F}}$ (taking into account water depth, draft and running sinkage at the fore) is calculated.

388 *Table 3 – Influence of $Fr_{ukc,F}$ on the repulsive contribution of the lateral force at the fore perpendicular for a wide range of*

389 *water depths for ship model A01, in the FH towing tank (cross section A) at lateral position y_0 = 2.5 m, velocity 0.728 m/s, fixed*

390 *propeller shaft 0 rpm.*

$\frac{T}{h_{\text{ship}} - T}$ (-)	Y_{F} (N)	Y_{A} (N)	h (m)	z_{F} (mm)	$Fr_{\text{ukc,F}}$ (-)	$Fr_{\text{ukc,F,crit}}$ (-)	$Fr_{\text{ukc,F}} - Fr_{\text{ukc,F,crit}} \geq 0$ (-)	$Y_{\text{F,ideal}}$ (N)	$Y_{\text{F}} - Y_{\text{F,ideal}}$ (N)
4.000	-2.10	3.36	0.1850	19.3	1.75	0.84	0.91	0.64	-2.74
3.333	-0.87	2.96	0.1924	17.8	1.42	0.84	0.58	0.57	-1.44
2.857	-0.56	2.69	0.1998	15.9	1.23	0.84	0.39	0.52	-1.07
2.500	-0.23	2.55	0.2072	14.7	1.10	0.84	0.26	0.49	-0.72
2.000	0.02	2.12	0.2220	14.7	0.95	0.84	0.11	0.41	-0.39
0.833	0.25	1.33	0.3256	9.9	0.57	0.84	0	0.25	0

391

392 For the ship models considered here, a critical non dimensional speed $Fr_{\text{ukc,F,crit}}$ exists between 0.57 and
393 0.95 where the space below the keel starts to block the flow to evacuate. In this example $Fr_{\text{ukc,F,crit}}$ has
394 been considered to be equal to 0.84 (following the analogy with equation (64)). If there would still be
395 sufficient possibility to evacuate, Y_{F} would continue having the same linear proportionality with Y_{A} (or
396 $\frac{T}{h_{\text{ship}} - T}$) and remain a (positive) attraction force. This is the case for an ideal fluid and has been represented
397 as $Y_{\text{F,ideal}}$ in the above table. The difference between the measured sway force and ideal sway force ($Y_{\text{F}} -$
398 $Y_{\text{F,ideal}}$) is then the repulsive contribution due to the limited space below the keel. This contribution has
399 been isolated and represented in Figure 10.

400

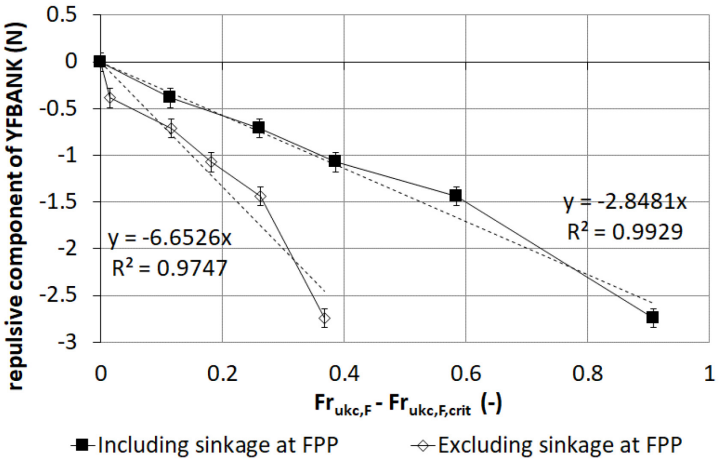

401

402 *Figure 10 - The repulsive contribution of the lateral force at the fore perpendicular as a function of the exceedance* $Fr_{ukc,F} -$

403 $Fr_{ukc,F,crit}$*, ship model A01, in the FH towing tank (cross section A) at lateral position* y_0 *= 2.5 m, velocity 0.728 m/s, fixed*

404 *propeller shaft 0 rpm*

405 One can clearly appreciate the linear trend between the exceedance of $Fr_{\mathrm{ukc,F}}$ and the repulsive

406 contribution. It is crucial that the forward sinkage is included, as indicated by the second example on the

407 figure.

408 The new mathematical model formulation is consequently:

409

410
$$Y_{\mathrm{F,BANK}} = \begin{cases} Fr_{\mathrm{ukc,F}} \le Fr_{\mathrm{ukc,F,crit}} & \xi_{Y_F} \Delta \; d_{2\mathrm{b}}^{-1} \; Tu_m\left(V_{\mathrm{eq},Y_F}\right) \\ Fr_{\mathrm{ukc,F}} > Fr_{\mathrm{ukc,F,crit}} & \xi_{Y_F} \Delta \; d_{2\mathrm{b}}^{-1} \; Tu_m\left(V_{\mathrm{eq},Y_F}\right) \left(1 + \xi_{Fr_{\mathrm{ukc,F}}}\left(Fr_{\mathrm{ukc,F}} - Fr_{\mathrm{ukc,F,crit}}\right)\right) \end{cases} \tag{60}$$

411

412 Note that at high exceedances, the linear relationship will no longer be valid (see the limitations of the

413 model, discussed in section 4.5).

414 The total bank induced force is then:

415
$$Y_{\mathrm{BANK}} = Y_{\mathrm{F,BANK}} + Y_{\mathrm{A,BANK}} \tag{61}$$

Because of the sign reversal of $Y_{\mathrm{F,BANK}}$, Y_{BANK} does not increase monotonously with increasing ship bank interaction, whereas K_{BANK} does. A constant proportionality with $Y_{\mathrm{A,BANK}}$, which also increases monotonously with increasing ship bank interaction, seems adequate and sufficient to capture the ship bank interaction for the heel moment:

$$K_{\mathrm{BANK}} = \xi_K T Y_{\mathrm{A,BANK}} \tag{62}$$

Recall that both are the result of the changed flow field in between the ship and the bank, but that K_{BANK} is dominantly driven by the hydrostatic disequilibrium that originates from it.

The bank induced yaw moment is then:

$$N_{\mathrm{BANK}} = \frac{L_{\mathrm{PP}}}{2} Y_{\mathrm{F,BANK}} - \frac{L_{\mathrm{PP}}}{2} Y_{\mathrm{A,BANK}} \tag{63}$$

4.5 Limitations of the mathematical model

The above mathematical formulations are not valid for the entire tested range. The following limitations are applicable:

- The model formulations are only applicable for parallel sailing at forward speeds along a steady environment.
- As depicted in Lataire (2014) the mathematical models are valid for subcritical speeds, which in practice is governed by the limit:

$$Fr_h \leq 0.84 Fr_{h,\mathrm{crit1}} \tag{64}$$

- For very small gaps interference between the boundary layer of the ship and the boundary layer on the obstacle can occur, which can have a significant effect on the lateral forces, see Lataire et al. (2023). For the present model test set, it means that 10% ukc should be excluded from Table 2, or similar centimetre gaps between the side of the ship and the closest obstacle. In order to cope with this effect, the method proposed by Lataire (2014) can be used, which essentially proportionally decreases the lateral force with penetration rate into the boundary layer. For instance, for a very small under keel clearance the following correction is appropriate:

$$Y_{\mathrm{A}} = \begin{cases} \xi_{Y_A} \Delta d_{2\mathrm{b}}{}^{-1} T u_m(V_{\mathrm{eq},Y_A}) & h_{\mathrm{ship}} - C_{\mathrm{M}}\, T - z_{\mathrm{A}} \geq \delta_{\mathrm{BLI,A}} \\ \dfrac{h_{\mathrm{ship}} - C_{\mathrm{M}}\, T - z_{\mathrm{A}}}{\delta_{\mathrm{BLI,A}}} \xi_{Y_A} \Delta d_{2\mathrm{b}}{}^{-1} T u_m(V_{\mathrm{eq},Y_A}) & h_{\mathrm{ship}} - C_{\mathrm{M}}\, T - z_{\mathrm{A}} < \delta_{\mathrm{BLI,A}} \end{cases} \tag{65}$$

For further considerations on δ_{BLI}, the reader is referred to Lataire et al. (2023).

4.6 Computation of the coefficients

The mathematical model is computed through regression analysis on the subset within the limitations mentioned in 4.5. The computations have been carried out based on ODRPack, an open source routine that was internally further developed towards present C# code, with the Math.NET library, although the mathematical concepts are still according to Boggs and Rogers (1990).

Per ship and per loading condition, but for all cross sections, the following coefficients need to be determined:

- X: 3 coefficients: $\xi_{y,X}$, $\xi_{VT,X}$, ξ_X
- Y_A : 3 coefficients: $\xi_{y,Y}$, ξ_{VT,Y_A}, ξ_{Y_A}
- Y_F : 4 coefficients : ξ_{VT,Y_F}, ξ_{Y_F}, $\xi_{Fr_{\mathrm{ukc,F}}}$ and $Fr_{\mathrm{ukc,F,crit}}$
- First alternative for the squat:
    - Z: 3 coefficients: $\xi_{y,Z}$, $\xi_{VT,Z}$, ξ_Z
    - M: 3 coefficients: $\xi_{y,M}$, $\xi_{VT,M}$, ξ_M
- Second alternative for the squat:
    - Z_F: 3 coefficients: ξ_{y,Z_F}, ξ_{VT,Z_F}, ξ_{Z_F}
    - Z_A: 3 coefficients: ξ_{y,Z_A}, ξ_{VT,Z_A}, ξ_{Z_A}
- K : 1 coefficient : ξ_K

The coefficient ξ_z is a constant. Note that for each degree of freedom a dedicated ξ_y provides better results as the sensitivity to the lateral restriction depends of the degree of freedom. For Y_A and Y_F, the same set can be used. Y_F, not only depends on Y_A, but also on Z_F (to determine the sinkage at the forward perpendicular). K depends only on Y_A.

4.7 Performance of the mathematical model

In this section the performance and limitations of the mathematical model will be demonstrated with some examples. Observe that in some previously shown figures the modelled values have been plotted as well. One can appreciate that for these examples provided sufficient accuracy is obtained with the limited set of coefficients.

A point of attention is the definition of the open water contribution. For a rather large ship model as T0Z, even in an open tank environment the walls are already felt. In such case, it is hard to predict the real

480 open water contribution. Figure 7 shows the model, assuming that in the cross section A an open water
481 contribution is obtained (marked as 'model open' in the legend). The ship bank interaction will add an
482 additional confinement on top of it (marked as 'model confined' in the legend). The solution of this
483 iterative problem is left for future research, but is similar as depicted by Raven (2019) for the resistance.

484 The following figures will show some additional examples concerning the results of ship models that have
485 not been discussed so far. For commercial reasons the ordinate axes and uncertainty intervals are masked,
486 but the proportionality of all datapoints is maintained. The cross section is drawn in the background. In
487 Figure 11 the ship-bank interaction forces for all degrees of freedom are shown for the inland vessel B01
488 sailing in cross section R:

489 • The bank induced surge force, Figure 11a, seems in this case somewhat underpredicted, yet at
490 severe eccentricities the mathematical model is closer to the measurements, even overpredicts
491 them.
492 • The difficult transition from attraction to repulsion for the forward lateral force seems well
493 captured in this case, Figure 11b, the rather large offset at 20% ukc in the centre of the cross
494 section should be assigned to a measurement failure.
495 • The trends for the lateral force at the aft are also well captured, Figure 11c. The difficult transition
496 at severe eccentricities is visible for 20% and 35% ukc (left hand side of the figure), where the
497 measured lateral force at the aft does not increase further, but drops.
498 • The prediction trends for the sinkage, Figure 11d-e, are also well followed, however an
499 underprediction is noted at one side, while at the other side the sinkage is overpredicted.
500 • The roll moment , Figure 11f, is sufficiently well predicted, given the fact that only one coefficient
501 is used. Again it is harder to obtain correct magnitudes at extreme eccentricities.

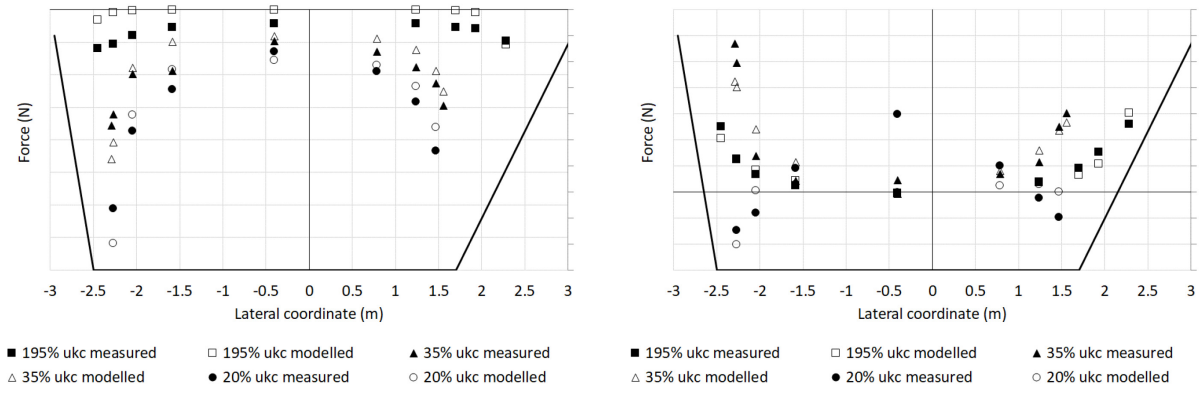

a. X b. Y_{F}

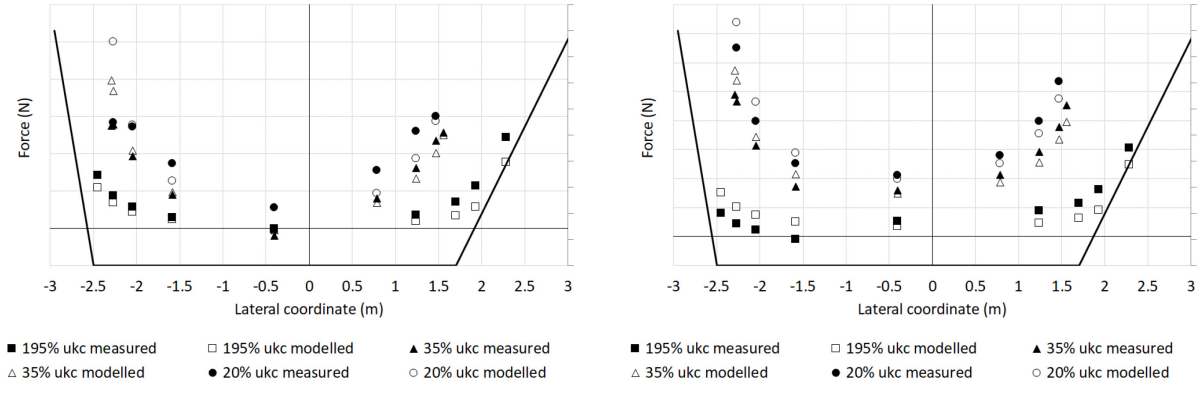

c. Y_{A} d. Z_{F}

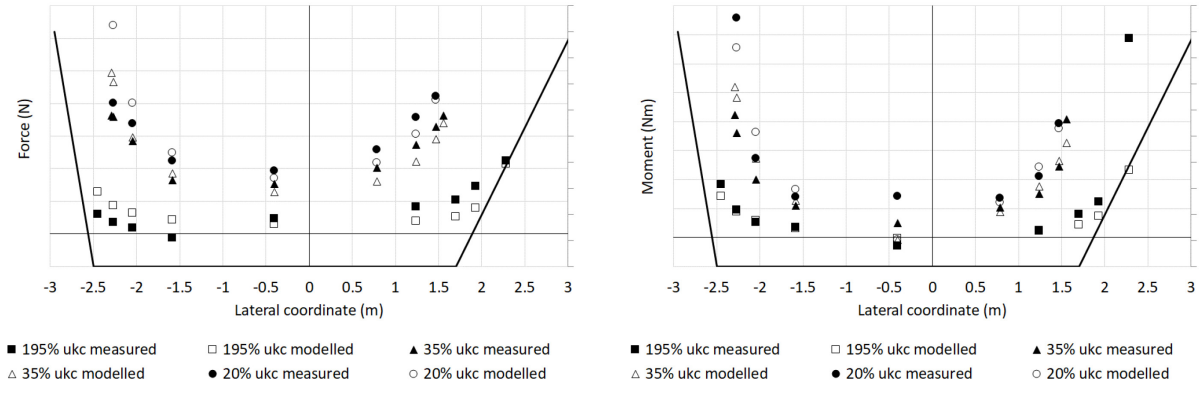

e. Z_{A} f. K

Figure 11 – Comparison between measured and modelled ship bank interaction forces in different degrees of freedom, ship B01, Cross section R, 0 rpm, 10.8 km/h (5.8 knots)

Figure 12 presents some results in case of a submerged bank, namely cross section O, with the container ship C0U01. In particular the attention is again drawn to the severe shift from attraction to repulsion for the lateral force at the forward perpendicular. It is hard to have a correct prediction when this shift happens, in this specific case the mathematical model seems to have a delay in the transition from attraction to repulsion with respect to the measurements and both at fore (F) and aft (A). For the lateral force at the aft, the trends are well captured. The measured repulsive forces at small eccentricities are questionable. The trends for the sinkage are also well captured, except that the measurements seem to indicate smaller sinkages at the centre of the section than the ones predicted by the mathematical model.

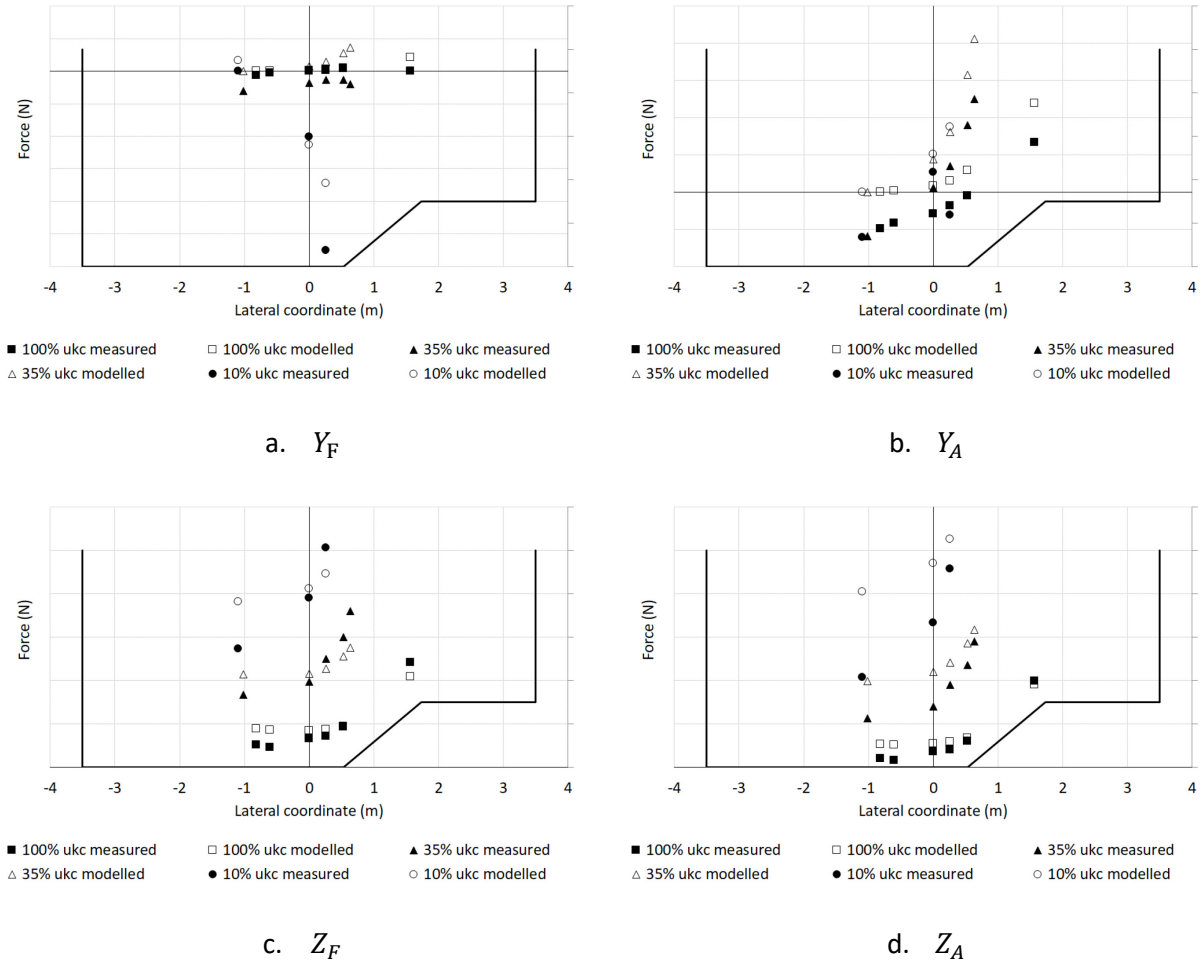

a. Y_{F} b. Y_A

c. Z_F d. Z_A

Figure 12 – Comparison between measured and modelled ship bank interaction forces in different degrees of freedom, ship C0U01, Cross section O, 0 rpm, 10 knots

As it is difficult to present the results for each degree of freedom, each ship and each cross section (given the additional fact that tests were conducted at different speeds and propeller rates), an alternative way is presented in Table 4 that lists all correlation coefficients between predictions and measurements for all tests and degrees of freedom considered. For a common open water manoeuvring model a sufficient accuracy is obtained whenever the correlation coefficient is larger than 0.9. This is almost always the case for the sinkage of the ship, but some obvious exceptions are noted for the other degrees of freedom. These can be explained as follows:

- The surge force due to ship-bank interaction is rather small compared to the resistance of the ship, except when high eccentricities or small blockages are concerned. This is the case for T0Z, and acceptable correlation ratios are seen in such case. For the other cases, the small measured values lead to severe offsets, however as shown in Figure 11a, an R^2-value of only 0.1573 does not necessarily imply a wrong mathematical model.
- For the lateral forces, the main culprits for smaller R^2-values are the correct prediction of the shift between attraction and repulsion (Y_F) or the severe eccentricities.
- The correlation for the roll moment is surprisingly well given the fact that only one coefficient is used.

Table 4 – R^2 correlation coefficients between measured and modelled ship-bank interaction forces

Ship	# tests	X	Y_F	Y_A	Z_F	Z_A	K
A01	250	0.52	0.73	0.90	0.90	0.87	0.84
B01	552	0.16	0.60	0.83	0.90	0.87	0.70
C0P	425	0.59	0.94	0.82	0.90	0.86	0.49
C0U01	1321	0.28	0.60	0.92	0.95	0.94	0.60
C0U03	1580	0.56	0.64	0.79	0.91	0.87	0.72

Ship	# tests	X	Y_F	Y_A	Z_F	Z_A	K
G0M	1254	0.64	0.54	0.90	0.86	0.85	0.74
T0Z	572	0.84	0.76	0.86	0.94	0.93	0.76
T0102	340	0.85	0.47	0.83	0.92	0.94	0.88
T0103	340	0.85	0.82	0.66	0.91	0.94	0.79

531

532 Finally, because the total hydrodynamic forces matter that act on the ship, a comparison for the total
533 measured and modelled forces is shown in Figure 13. The trends of the total surge force are well captured,
534 although an offset is noted. A similar offset is observed for the lateral force, but there again the drop in
535 measured force at extreme eccentricities is hard to predict. Although the lateral force drops, the roll
536 moment is still increasing at the same point. The squat of the ship is well predicted, except for the pitch
537 which is significantly underestimated at the extreme eccentricity. The trend for the yaw moment is well
538 captured, but slightly underestimated.

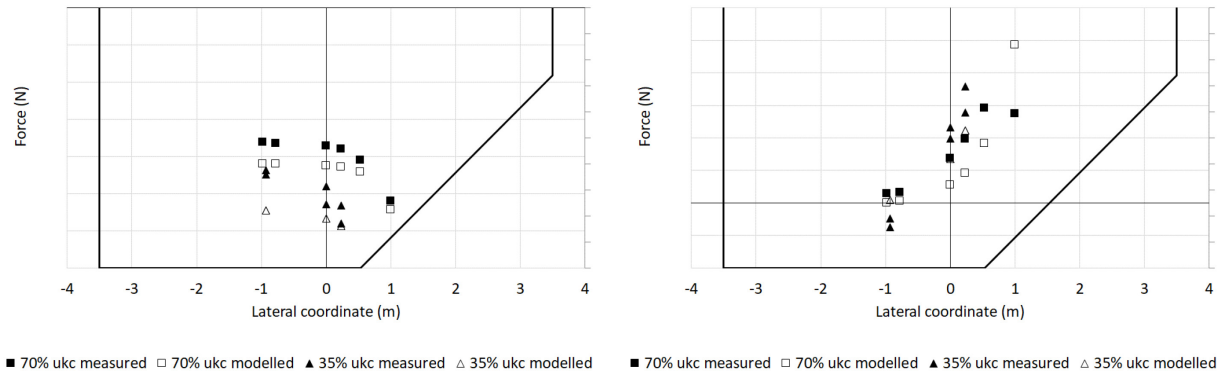

a. X b. Y

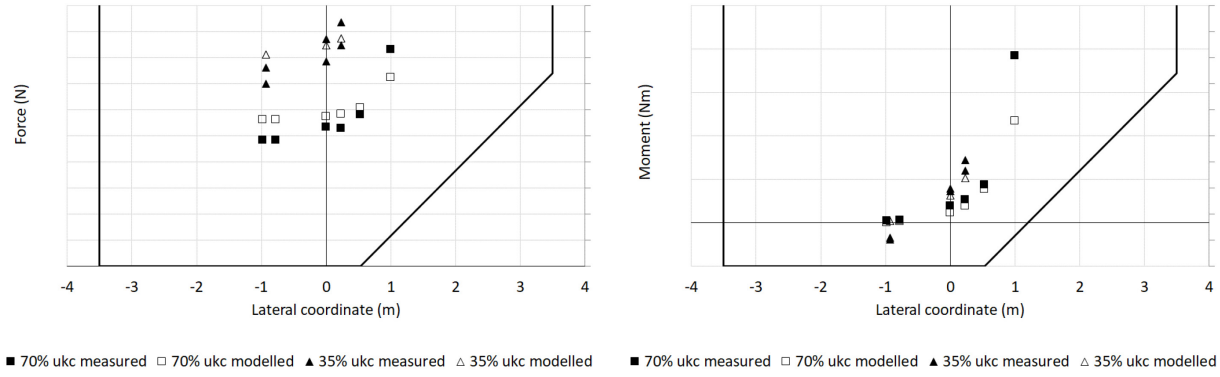

c. Z

d. K

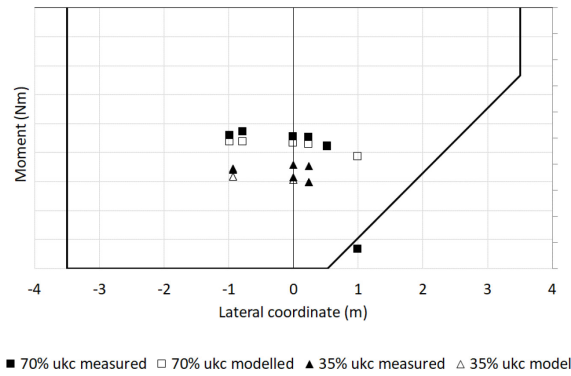

e. M

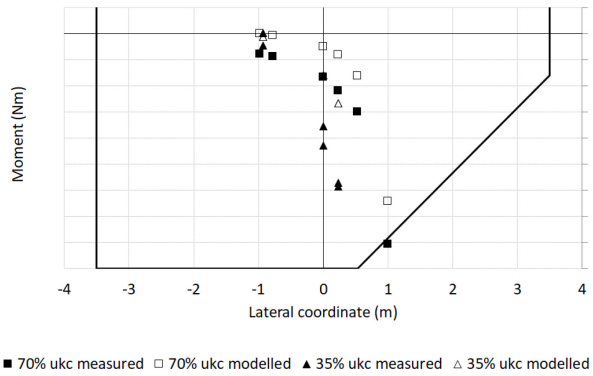

f. N

Figure 13 – Comparison between measured and total modelled hydrodynamic forces in different degrees of freedom, ship G0M, Cross section N, 0 rpm, 10 knots

5 Conclusions

The present paper discussed a 6 DOF manoeuvring model to predict the effects of a channel cross section and the eccentric position of the ship in that channel to the hydrodynamic behaviour of the ship. This so-called ship bank interaction is mainly governed by the following parameters:

- the velocity of the ship V;
- the space below the keel or under keel clearance;

- the space in between the bank and the ship or the distance to the bank,
- which in turn depends on the layout of the bank, from a simple linear slope to an irregularly shaped profile.

and can be summarized as follows in case of moderate conditions:

- A resistance increase in the longitudinal direction.
- A sway force directed towards the closest bank. The resultant is located in the aft part of the ship, hence creating a yaw moment that direct the bow away from the closest bank.
- An increase of the squat of the ship, i.e. increased midship sinkage and altered trim behaviour.
- A heel of the ship so that the upper part of the ship heels towards the closest bank.

The background of the mathematical model is a comprehensive database of multiple ship models that were tested in multiple cross sections since 2006 in the Towing Tank for Manoeuvres in Confined Water. The previously published concept of weighting the cross section to derive an equivalent blockage and ship bank interaction parameter was here reused to update the formulation of the lateral force at the forward perpendicular and to extend the predictions towards all 6 degrees of freedom. Although the vertical DOF tend to be neglected in manoeuvring in confined water, the ship bank contribution is certainly not negligible in all degrees of freedom. A rather limited set of regression coefficients is needed to be able to predict the effect of the cross section on the ship's hydrodynamics. This choice for a limited set was made for robustness and genericity. Obviously better predictions can be obtained with dedicated sets or extended sets of coefficients, but this was not the aim.

A further point of attention is the correct split up between the behaviour of the ship in open water and the behaviour of the ship in a cross section. Because of the influence width, this split up is not always possible. A rather large ship model, such as KVLCC2 will already feel the presence of the tank walls if no obstacles are present. This part of the research is left for future work.

571 At the same time it is the intention of the authors to investigate whether the mathematical formulations
572 can be extended to cope with the behaviour of a drifting ship in any cross section.

573

574 6 References

575 Boggs, P.T., Rogers, J.E. (1990). The computation and use of the asymptotic covariance matrix for
576 measurement error models. Internal Report 89-4102 Applied and Computational Mathematics Division.
577 National Institute of Standards and Technology, Gaithersburg, MD.

578 Ch'ng, P.W., Doctors, L.J. & Renilson, M.R. (1993). A method of calculating the ship-bank interaction forces
579 and moments in restricted water. International Shipbuilding Progress, 40(421), pp.7–23.

580 Delefortrie, G.; Eloot, K.; Lataire, E.; Van Hoydonck, W.; Vantorre, M. (2016a). Captive model tests based
581 6 DOF shallow water manoeuvring model, 4th MASHCON conference, Hamburg, Germany

582 Delefortrie, G., Geerts, S., Vantorre, M., (2016b). "The towing tank for manoeuvres in shallow water",
583 Proceedings of the 4th International Conference on Ship Manoeuvring in Shallow and Confined Water
584 with Special Focus on Ship Bottom Interaction, Hamburg, Germany, 23 to 25 May 2016 (4th MASHCON).
585 pp. 226-235.

586 Delefortrie, G., Sotelo, M., Boucetta, D. (2022) Practical Squat Assessment for a Ship Manoeuvring in
587 Muddy Environments. Applied Ocean Research, 123, 103181,
588 https://doi.org/10.1016/j.apor.2022.103181

589 Delefortrie, G., Eloot, K., Lataire, E. (2023). The influence width of drifting ships. Applied Ocean Research,
590 141, 103779. https://doi.org/10.1016/J.APOR.2023.103779 .

591 Delefortrie, G., Verwilligen, J., Vantorre, M., Lataire, E. (2024). Exact and approximated solutions to the
592 critical ship speed in canals, 35th PIANC World Congress, Cape Town, South-Africa.

Fuehrer, M. (1978). The results of systematic investigations into lateral forces for determining the effects of hydraulic asymmetry and eccentricity on the navigation of sea-going ships in canals. In Symposium on aspects of navigability. pp. 1–18.

Fujino, M., (1968). Experimental studies on ship manoeuvrability in restricted waters part i. International Shipbuilding Progress, 15(168), pp.279–301.

Hadi, E.S., Tuswan, T., Azizah, G., Ali, B., Samuel, S., Hakim, M.L., ... Satrio, D. (2023). Influence of the canal width and depth on the resistance of 750 DWT Perintis ship using CFD simulation. Brodogradnja, 74 (1), 117-144. https://doi.org/10.21278/brod74107

ITTC (2021) Recommended Procedures and Guidelines. Uncertainty analysis for manoeuvring predictions based on captive manoeuvring tests. https://www.ittc.info/media/9687/75-02-06-04.pdf (Accessed May 2024).

Kaidi, S., Smaoui, H. & Sergent, P. (2017) Numerical estimation of bank-propeller-hull interaction effect on ship manoeuvring using CFD method. J Hydrodyn 29, 154–167. https://doi.org/10.1016/S1001-6058(16)60727-8

Kim, Y.K., Ng, E.Y.K. (2017) CFD-study of ship-to-bank interaction. Trans RINA, Vol 159, Part A3, Intl J Maritime Eng, Jul-Sep 2017, p 281 – 290. DOI No: 10.3940/rina.ijme.2017.a3.426.

Lataire, E., Vantorre, M., Delefortrie, G. (2012) A prediction method for squat in restricted and unrestricted rectangular fairways. Ocean Engineering, Vol. 55, pp. 71-80. https://doi.org/10.1016/j.oceaneng.2012.07.009

Lataire, E. (2014) Experiment Based Mathematical Modelling of Ship-Bank Interaction, PhD-thesis, Faculty of Engineering and Architecture, Ghent University, ISBN 978-90-8578-748-8.

614 Lataire, E., Vantorre, M., Delefortrie, G. (2015), Longitudinally Directed Bank Effects, MARSIM 2015,
615 Newcastle, UK.

616 Lataire, E., Delefortrie, G., & Vantorre, M. (2016a). Impact of banks on ship squat (K. Uliczka, C.-U. Böttner,
617 M. Kastens, K. Eloot, G. Delefortrie, M. Vantorre, … E. Lataire, Eds.). https://doi.org/10.18451/978-3-
618 939230-38-0_15

619 Lataire, E., Vantorre, M., Delefortrie, G. (2018). The influence of the ship's speed and distance to an
620 arbitrarily shaped bank on bank effects. J. Offshore Mech. Arct. Eng. 140(2): [1-11].
621 https://hdl.handle.net/10.1115/1.4038804

622 Lataire, E., Raza, A., Vantorre, M., Delefortrie, G. (2023) Boundary layer influence on ship model tests in
623 extremely shallow and confined water. Journal of Hydrodynamics, https://doi.org/10.1007/s42241-023-
624 0024-0

625 Lee, S. (2023) Hydrodynamic interaction forces on different ship types under various operating conditions
626 in restricted waters, Ocean Engineering, Vol. 267, 113325,
627 https://doi.org/10.1016/j.oceaneng.2022.113325.

628 Liu, G., Ma, N., Gu, X. (2021) CFD prediction of ship-bank interaction for KCS under extreme conditions.
629 Journal of Marine Science and Technology (2021) 26:1062–1077. https://doi.org/10.1007/s00773-021-
630 00798-x

631 Luo, W. , Yang, B., Sun, Y. (2021) Hydrodynamic Analysis of KVLCC2 Ship Sailing near Inclined Banks.
632 Mathematical Problems in Engineering, Volume 2021, Article ID 6655971, 16 pages
633 https://doi.org/10.1155/2021/6655971

634 Newman, J.N., (1965). The force and moment on a slender body of revolution moving near a wall. ,
635 (December 1965), pp.1–17.

636 Norrbin, N.H. (1974). Bank effects on a ship moving through a short dredged channel. In R. D. Cooper & S.
637 W. Doroff, eds. 10th ONR. Office of Naval Research, pp. 71–88.

638 Norrbin, N.H. (1985). Bank clearance and optimal section shape for ship canals. In 26th International
639 Navigation Congress. PIANC, pp. 167–178.

640 Raven, H., (2019) Shallow-water effects in ship model testing and at full scale, Ocean Engineering, Vol.
641 189, 106343.

642 Schoenherr, K.E., (1960). Data for estimating bank suction effects in restricted water and on merchant
643 ship hulls. In 1st Symposium on ship maneuverability. SNAME, pp. 199–210

644 Tuck, E.O. (1966). Shallow-water flows past slender bodies. J. Fluid Mech. 26: pp. 81–95

645 Van Hoydonck, W., Toxopeus, S., Eloot, K., Bhawsinka, K., …, Visonneau, M., (2019). Bank Effects for
646 KVLCC2, Journal of Marine Science and Technology, Vol. 24, No.1, pp. 174–199.

647 Yuan, Z.M. (2019) Ship Hydrodynamics in Confined Waterways, Journal of Ship Research, Vol. 63, N° 1, p
648 16-29.